atmosphere

MDPI

Article

Transformation and Migrant Mechanism of Sulfur and Nitrogen during Chemical Looping Combustion with $CuFe_2O_4$

Haichuan Li, Ziheng Han, Chenye Hu, Jingjing Ma * and Qingjie Guo *

State Key Laboratory of High-Efficiency Utilization of Coal and Green Chemical Engineering, Ningxia University, Yinchuan 750021, China; haichuanlicq@163.com (H.L.); hanziheng0531@163.com (Z.H.); hu13986940198@163.com (C.H.)

* Correspondence: majingjing@nxu.edu.cn (J.M.); qingjie_guo@nxu.edu.cn (Q.G.); Tel./Fax: +86-951-2062323 (J.M. & Q.G.)

Abstract: Chemical looping combustion (CLC) is a key technology for capturing CO_2. Different types of oxygen carrier (OC) particles are used in coal CLC. The migration and transformation behaviors of sulfur and nitrogen are basically the same when $CaFe_2O_4$ and Fe_2O_3/Al_2O_3 are used as OC. CLC can be divided into two reaction stages: coal pyrolysis and char gasification; SO_2 and NO show bimodal release characteristics, both of which show a basic trend of rising first and then falling down. The contents of H_2S and NO_2 increased rapidly at the beginning of the reaction and then decreased slowly at the stage of char gasification. H_2S is released rapidly during coal pyrolysis and discharged from the reactor with flue gas, and then part of H_2S is converted to SO_2 during the char gasification stage by OC particles. NO can be oxidized by OC particles and form NO_2. The increase in the reaction temperature and oxygen-to-carbon ratio (O/C) contributes to the release of sulfur and nitrogen and higher reaction temperature and O/C can inhibit the formation of metal sulfide. O_2 released by $CuFe_2O_4$ significantly increases the contents of SO_2, H_2S, NO and NO_2 in flue gas. This work is helpful for improving control strategies for pollutants.

Keywords: chemical looping combustion; sulfur; nitrogen; oxygen carrier particles

Citation: Li, H.; Han, Z.; Hu, C.; Ma, J.; Guo, Q. Transformation and Migrant Mechanism of Sulfur and Nitrogen during Chemical Looping Combustion with $CuFe_2O_4$. *Atmosphere* **2022**, *13*, 786. https://doi.org/10.3390/atmos13050786

Academic Editor: Jaroslaw Krzywanski

Received: 15 April 2022
Accepted: 9 May 2022
Published: 12 May 2022

1. Introduction

Fossil fuel combustion inevitably leads to CO_2 emissions, which are the main factor of land desertification and the greenhouse [1,2]. Reducing CO_2 emissions is the most effective way to solve global warming. CCUS (Carbon Capture, Utilization and Storage) technology is the key technology to reduce CO_2 emissions and improve CO_2 utilization, and has attracted wide attention [3]. Chemical looping combustion (CLC) is considered to be one of the best carbon capture method in the world [4–6]. CLC uses lattice oxygen/molecular oxygen provided by oxygen carrier (OC) particles to oxidize fuel instead of air, which can avoid the generation of thermodynamic nitrogen oxides [7]. CLC can realize the self-heating operation [8]. The OC can release lattice oxygen/O_2 in a fuel reactor (FR) and then it can be transferred to an air reactor (AR) for oxidative regeneration. Additionally, a large amount of heat can be released when reduced OC reacts with air. [9]. When steam is used as a gasification agent in CLC high concentration of CO_2 can be obtained by condensing steam at the outlet of the FR. Therefore, CLC also has the advantage of internal separation of CO_2. OC particles are an important link connecting the two reactors, it has the functions of loading heat and oxygen which plays an important role in the process of CLC [10]. At present, most OC particles are transition metal oxides. Among them, iron-based OC are widely used because of their low price, non-toxicity and stable cycle performance [11]. However, iron-based OC also exhibit a poor oxygen transformation performance. Copper-based OC are widely used in industry due to their better oxygen release characteristics [12]. However, it is easy to agglomerate at high temperatures, resulting in poor cycling stability. In order to solve the disadvantage of single metal OC,

the development and utilization of bimetallic OC has attracted the attention of scholars [13]. Copper ferrite has the dual advantages of CuO and Fe_2O_3, which can release both lattice oxygen and molecular oxygen [4]. The existence of an iron phase in OC particles can significantly improve the stability [14]. Therefore, $CuFe_2O_4$ has wide application prospects in the process of CLC.

Compared with traditional combustion, coal CLC has many advantages, for example, realizing energy cascade utilization. However, in the complex structure and composition of coal, a large number of pollution elements such as sulfur and nitrogen and also trace elements such as Hg, As and Se can be found [15]. The release of pollutants cannot be avoided in the process of coal CLC [16,17]. The release of sulfur and nitrogen not only has a strong corrosive effect on equipment and pipelines, but also affects the storage and utilization of CO_2. During CLC, the structure and oxygen release mode of OC can affect the migration and transformation behavior of sulfur and nitrogen in coal. Reaction conditions such as the reaction temperature and O/C (oxygen-to-carbon ratio) also have a significant impact on the fate of sulfur and nitrogen. Jinchen Ma et al. [18] found that Fe_2O_3/Al_2O_3 OC prepared by the sol–gel process had strong resistance to sulfur during in situ coal CLC and sulfur-containing substances were not detected on the surface of OC particles after reaction, and a low O/C could promote the formation of H_2S. Because of its good reactivity, copper-based OC can promote the release of sulfur-containing substances and promote the conversion of H_2S to SO_2. The migration and transformation behavior of nitrogen is related to the oxygen-releasing mode of OC. OC such as Fe_2O_3 and NiO are used in coal CLC. Only N_2 can be detected at the outlet of the FR without NOx (NO, NO_2, and N_2O) formation because of the release of lattice oxygen, and NO can be detected only in the AR [19]. When a copper-based OC is used, the molecular oxygen released by the OC particles can promote the formation of NO, which makes the CLC tend towards traditional combustion [20]. Similar to the release mechanism of sulfur, the increase in O/C and reaction temperature can promote the conversion of fuel nitrogen to N_2 and NO [21]. Therefore, in the process of coal CLC, it is of great significance to explore the effects of OC particles with different oxygen release mode and reaction conditions on the migration and transformation of sulfur and nitrogen pollutants.

In this study, coal CLC experiments were carried out on a batch fluidized bed with Ningxia bituminous coal (NX coal) as fuel. Different OC particles (Fe_2O_3/Al_2O_3 and $CuFe_2O_4$) were prepared by the mechanical mixing method to explore the fate of sulfur and nitrogen during CLC. By changing the reaction temperature and O/C, we explored the effect of reaction conditions on the migration and transformation mechanism of sulfur and nitrogen. Finally, ten cycles of experiments carried on the batch fluid bed and the cyclic stability of the two kinds of OC particles is discussed. We also confirm the reaction mechanism of OC particles on sulfur and nitrogen during the cyclic experiment.

2. Materials and Methods

2.1. Coal Sample and Oxygen Carrier Particles

In our experiment, bituminous coal from Ningxia, China, was used as fuel. The contents of sulfur and nitrogen in coal were 0.4006% and 1.46%, respectively. The results of the proximate analysis and ultimate analysis we carried out are shown in Table 1 and the coal samples were screened to 106–150 μm.

Table 1. The proximate analysis and ultimate analysis of NX coal.

Sample	Proximate Analysis wt.%				Ultimate Analysis wt.%				
	M	**A**	**V**	**FC**	**C**	**H**	**N**	**S**	**O**
NX	5.18	4.56	26.95	63.31	77.60	5.16	1.46	0.40	10.77

Two kinds of OC particles with different configurations were prepared by the mechanical mixing method. Firstly, 160 g Fe_2O_3 and 80 g CuO were weighed according to

n(Fe_2O_3):n(CuO) = 1:1, respectively. Additionally, 500 mL of deionized water was added to the colloid mill for mechanical mixing for 20 min. The mixed solution was vacuum filtered. The filter cake was oven dried at 150 °C for 24 h. Then, it was transferred to a muffle furnace at 900 °C and calcined for 6 h. Finally, $CuFe_2O_4$ particles were obtained and crushed to 150–270 μm. The preparation method of Fe_2O_3/Al_2O_3 is the same as that of $CuFe_2O_4$. It is necessary to note that the mass ratio of Fe_2O_3 and Al_2O_3 is 7:3 and the particle size of Fe_2O_3/Al_2O_3 is the same as $CuFe_2O_4$ particles.

An automatic physical chemistry adsorption instrument (Quantachrome, Anton Paar, Graz, Austria) was used to measure BET surface area of OC. Nitrogen was used as the adsorbate and helium was used as the carrier gas. The two gases were mixed in a certain proportion to reach the specified relative pressure, and then flowed over the OC. When the sample tube was heated in liquid nitrogen, the OC physically adsorbed nitrogen in the mixed gas, while the carrier gas was not adsorbed. Then, the BET specific surface area of the OC could be measured. X-ray diffraction (XRD, D8 ADVANCE A25, Bruker AXS, Karlsruhe, Germany) was used to determine the crystal phase of the OC particles.

2.2. Experimental Procedure

All experiments were conducted in a batch fluidized bed and the experimental device is shown in Figure 1. The specific description of the batch fluidized bed reactor (Figure S1) is consistent with previous work [22]. Additionally, the internal diameter of the fluidized bed is 60 mm and it is 1000 mm high. The mass of the NX coal was 0.5 g in all experiments. When O/C = 1, 3, 5 the mass of iron-based OC are 20 g, 40 g, and 100 g, respectively. The masses of $CuFe_2O_4$ are 12 g, 35.87 g, and 59.81 g, respectively.

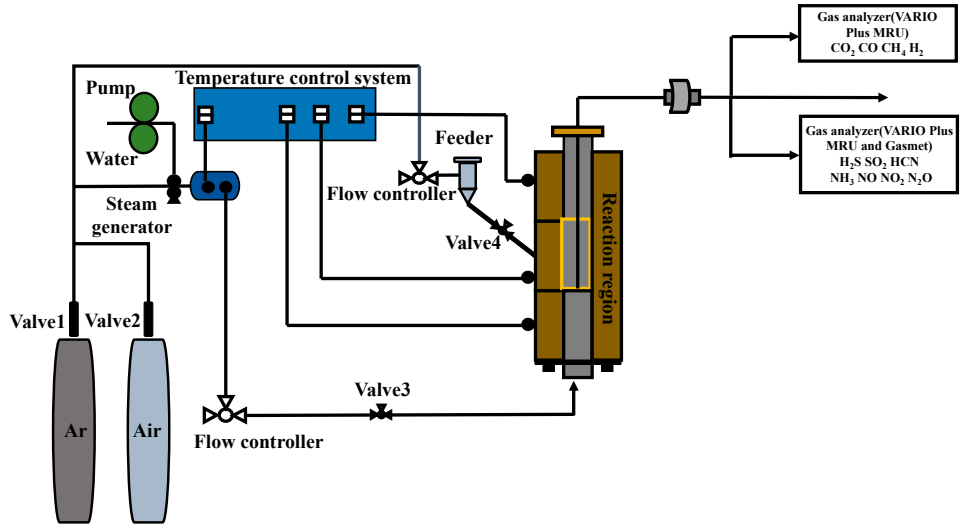

Figure 1. Experimental flow chart.

The experiment used Ar as the fluidizing gas; the volume flow rate was 1300 mL/min, the steam mass flow rate was 1.2 g/min, and the volume ratio of argon and steam was 1:1. The minimum fluidization velocity (U_{mf}) of the fluidized bed was 0.86 m/s, and the apparent gas velocity (U_0) was 1.2 times U_{mf}. The contents of CH_4, CO, CO_2, SO_2, NO, and NO_2 were measured online by a flue gas analyzer (DX4000, Gasmet, Finland, and the detection limit of selenium is 0.01 ppm), and the content of H_2S in flue gas was measured online by an H_2S flue gas analyzer (MRU VARIO PLUS, Germany) (Figure S2); the detection limit of selenium is 0.01 ppm. The reactor was heated to the reaction temperature and reaction temperature was controlled by three thermocouples in the temperature control system. Then, the feed was added to the feeder, allowing the samples to be transferred to the reactor by Ar. Then, valve4 was closed and valve3 was opened. The experimental batch fluidized bed is an isothermal reactor. The reaction then began. In order to ensure the

accuracy of the experimental results, the zero point of the flue gas analyzer was calibrated before the experiment and three groups of parallel experiments were carried out to ensure the reliability of the results.

The distribution of sulfur and nitrogen species of NX coal in flue gas was simulated by HSC Chemistry 6.0 when $CuFe_2O_4$ and Fe_2O_3/Al_2O_3 were used as the OC. The simulation temperature was 650–1000 °C and the O/C is from 1 to 10. The reaction equilibrium components were used and C, H, O, N, and S were converted into molar quantities according to the ultimate analysis of NX coal for calculation, as shown in Table 1.

2.3. Date Analysis

The volume flow rate of the outlet gas (F_{out}, L/min) is calculated by the mass balance of N_2 flow introduced:

$$F_{out} = \frac{F_{\text{in}}}{1-\sum X_i} \tag{1}$$

$$i = (\text{CO},\text{CH}_4,\text{CO}_2,\text{H}_2\text{S},\text{SO}_2,\text{NO},\text{NO}_2) \tag{2}$$

where F_{in} is the inlet volume flow rate of Ar, L/min, and *Xi* are the instantaneous volume fractions of CO, CH_4, CO_2, H_2S, SO_2, NO and NO_2 in the outlet gas flow on a dry basis, vol%.

The gas content (X_i, %) is calculated using the following:

$$X_i = \frac{\int_0^t F_{out} \cdot y_i \mathrm{d}t}{\int_0^t F_{out} \cdot (y_{\text{CO}} + y_{\text{CH}_4} + y_{\text{CO}_2} + y_{\text{CO}_2} + y_{H_2S} + y_{\text{SO}_2} + y_{\text{NO}_2} + y_{\text{NO}})\mathrm{d}t} \tag{3}$$

The molar number of coal is calculated as follows, where mcoal denotes the mass of coal, *C* means the content of carbon of NX coal, and M means the relative atomic mass of carbon

$$n_{\text{c}}, \text{coal} = \frac{m_{\text{coal}} \times C}{\text{M}} \tag{4}$$

The calculation method of carbon conversion during CLG is as follows:

$$X_{\text{C}} = \frac{\int_0^t n_{\text{out}} (X_{\text{CO}} + X_{\text{CO}_2} + X_{\text{CH}_4} + X_{\text{CO}_2} + X_{\text{H}_2\text{S}} + X_{\text{SO}_2} + X_{\text{NO}_2} + X_{\text{NO}})\mathrm{d}t}{n_{\text{c}}, \text{coal}} \tag{5}$$

The yield of per unit time of CO_2 is as follows:

$$\mathrm{d}X_{CO_2} = \frac{\Delta X_{CO_2}(t)}{\Delta t} \tag{6}$$

3. Results and Discussion

3.1. Thermodynamic Simulation of Fate of Sulfur and Nitrogen during CLC

The thermodynamic simulation software HSC Chemistry 6.0 was used to simulate the distribution of sulfur and nitrogen during coal CLC with NX coal. As shown in Figure 2a,b, the distribution of sulfur-containing substances in the process of coal CLC with two type of OC was simulated at 850 °C. SO_2 was the main gaseous sulfur-containing substance and the content of SO_2 increased with the increase in O/C. Due to the increase in O/C, OC particles can provide more lattice oxygen [6]. H_2S was oxidized by OC particles, which resulted in the content of SO_2 increasing. It can be found that the content of H_2S gradually decreased with the increase om O/C and when O/C was fixed to 5 the content of H_2S was 0, as shown in Figure 2a. For $CuFe_2O_4$, the content of Cu_2S and H_2S decreased with the increase in O/C. Therefore, when O/C increases, the content of SO_2 also increases. This is because an increase in O/C can promote the oxidation of H_2S to SO_2, as shown in Figure 2b. Therefore, $CuFe_2O_4$ can effectively inhibit the formation of metal sulfide when O/C exceeds 5. A higher O/C can inhibit $CuFe_2O_4$ deactivation due to sulfur poisoning. In the process of coal CLC, minerals in coal can interact with sulfur to fix it and form alkali

metal sulfate [23]. With the increase in O/C, the fixation effect of minerals in coal on sulfur is gradually enhanced. As mentioned above, when O/C is fixed to 5, OC particles have strong interactions with sulfur in coal. Therefore, when O/C is fixed to 5, the variation of sulfur-containing substances during CLC at different reaction temperatures is simulated, as shown in Figure 3a,b. The content of SO_2 increased with the increase in temperature. With the increase in temperature, coal particles can react more completely, resulting in increased SO_2(g) release. It can be seen from Figure 3 that the formation of metal sulfides was inhibited with the increase in reaction temperature (the contents of $Fe_{0.877}S$, FeS and Cu_2S gradually decreased).

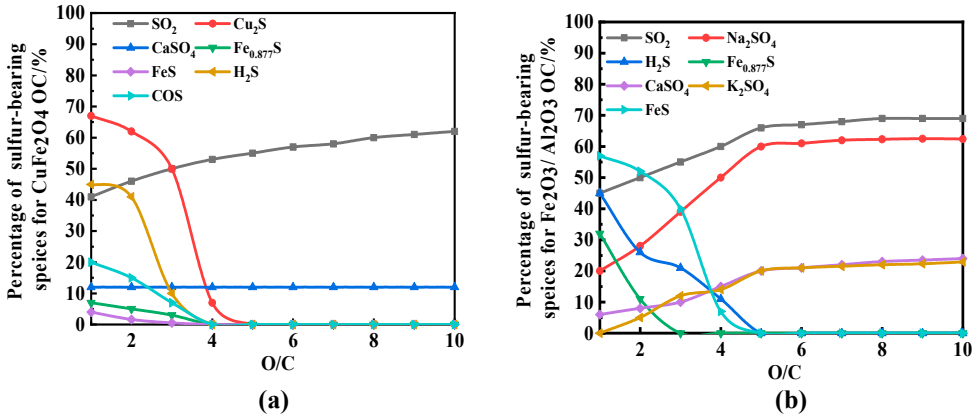

Figure 2. The variation trend of sulfur-containing substances during coal CLC with (**a**) $CuFe_2O_4$ and (**b**) Fe_2O_3/Al_2O_3 under different O/C.

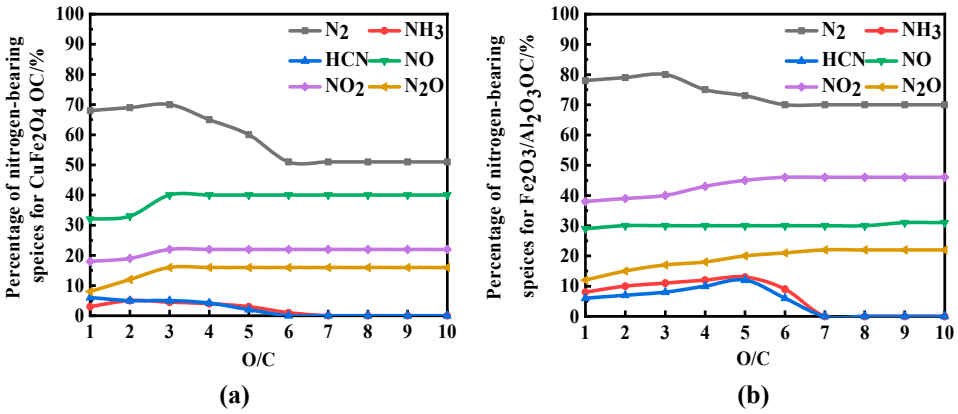

Figure 3. The variation trend of nitrogen-containing substances during coal CLC with (**a**) $CuFe_2O_4$ and (**b**) Fe_2O_3/Al_2O_3 with different O/C.

According to the thermodynamic simulation results, the migration and transformation behavior of fuel nitrogen during CLC is related to the oxygen release mode of OC particles. N_2 was the main form in the FR and its content decreased with the increase in O/C for iron-based OC and $CuFe_2O_4$, as shown in Figure 3. With the increase in O/C, the trend of OC particles converting fuel nitrogen into NOx gradually intensifies. Therefore, the NOx content gradually increased with the increase in O/C. Compared with iron-based OC, this can produce more N_2 and NOx. This is because $CuFe_2O_4$ can release molecular oxygen and promote the transformation of fuel nitrogen to N_2 and NOx [24,25]. We also observed similar phenomena in the fluidized bed experiment, which will be discussed in detail in the next section. When O/C was fixed to 5, with the increase in the reaction temperature, the content of N_2 and NOx increased gradually, while HCN and NH_3 increased first and then decreased, as shown in Figure 4. This is because the increase in the reaction temperature can promote the pyrolysis and gasification of coal, so that the fuel is

completely reacted. Therefore, when the temperature increased from 500 °C to 800 °C, the HCN and NH_3 contents increased with the increase in temperature, as shown in Figure 5. However, when the reaction temperature was higher than 800 °C, the content of HCN and NH_3 began to decrease, while the content of N_2 and NOx increased. This is because OC particles can promote HCN and NH_3 to be oxidized N_2 or NOx with an increasing reaction temperature [11].

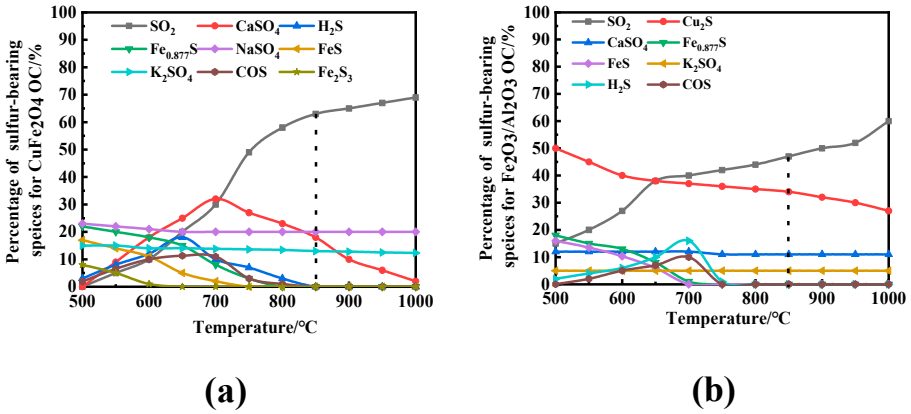

Figure 4. The variation trend of sulfur-containing substances during coal CLC with (**a**) $CuFe_2O_4$ and (**b**) Fe_2O_3/Al_2O_3 with different reaction temperatures.

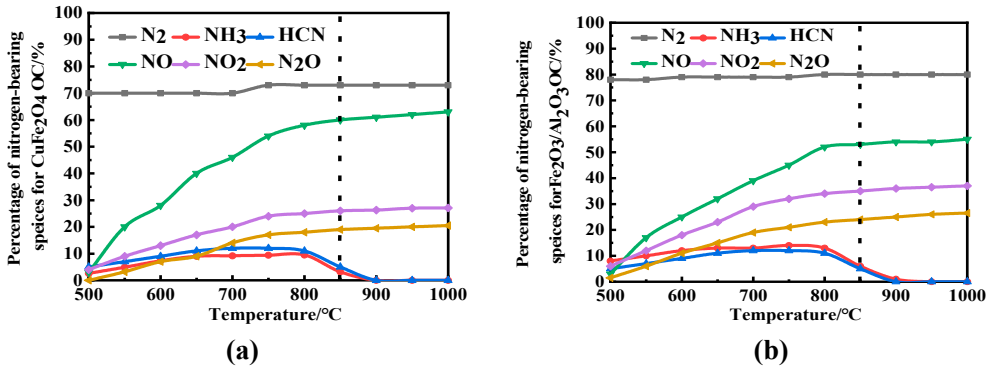

Figure 5. The variation trend of nitrogen containing substances during coal CLC with (**a**) $CuFe_2O_4$ and (**b**) Fe_2O_3/Al_2O_3 with different reaction temperatures.

3.2. Effect of Reaction Temperature and O/C on the Migration and Transformation Mechanism of Sulfur and Nitrogen during CLC

When iron-based OC and $CuFe_2O_4$ were used, the migration and transformation behaviors of sulfur in NX coal were basically the same and most of them were released in the form of SO_2 and H_2S. The oxygen release mode and structure of two types of OC particles were different. However, the releases of SO_2 and H_2S were basically the same, as shown in Figure 6. At different reaction temperatures with O/C = 5, SO_2 shows a bimodal release, which is because the CLC can be divided into two stages: the rapid pyrolysis of coal and gasification of coal char. In the process of the rapid pyrolysis of coal, the volatile matter of coal was removed, and the unstable thermodynamically bound sulfur (FeS_2) in coal would rapidly release and form H_2S and COS. Sulfur precursors (H_2S and COS) were rapidly oxidized by OC particles, resulting in the content of SO_2 increasing. SO_2 content decreased gradually at the end of the coal pyrolysis stage. Therefore, SO_2 content increased first and then decreased in the rapid pyrolysis stage of coal. However, the variation trend of SO_2 with time in the gasification stage of coal char was the same as that in the rapid pyrolysis stage of coal, and it still showed the basic trend of rising and then falling, but the overall release was less than that in the rapid pyrolysis stage of coal. This is because most of the sulfur in coal was released in a large amount during the process

of coal devolatilization in the thermodynamically unstable combination state and only a small part of sulfur was released in the gasification stage [25,26]. In Figure 6a–e, it can be seen that the content of SO_2 and H_2S increased with the increase in reaction temperature when Fe_2O_3 and $CuFe_2O_4$ were used as OC, which is consistent with the thermodynamic simulation results. This indicates that temperature can promote the decomposition of coal particles, and more coal was involved in the reaction to promote the release of SO_2 and H_2S. As shown in Figure 6a–e, $CuFe_2O_4$ can effectively promote the release of SO_2 and H_2S. This is because $CuFe_2O_4$ can release molecular oxygen, which promotes the decomposition of sulfur-containing components in coal to a certain extent. Unlike lattice oxygen, molecular oxygen can undergo gas–solid (coal/char particles) reactions and gas–gas reactions to promote the complete reaction of coal. The formation of Cu_2S was related to the reaction temperature. When the reaction temperature increased, the content of Cu2S decreased and the content of SO_2 increased. As shown in Figure 4, this may be due to the decomposition of Cu_2S at high temperature. In Figure 4b, it can be seen that the Cu_2S phase can be observed when the reaction temperature increased from 650 °C to 850 °C.

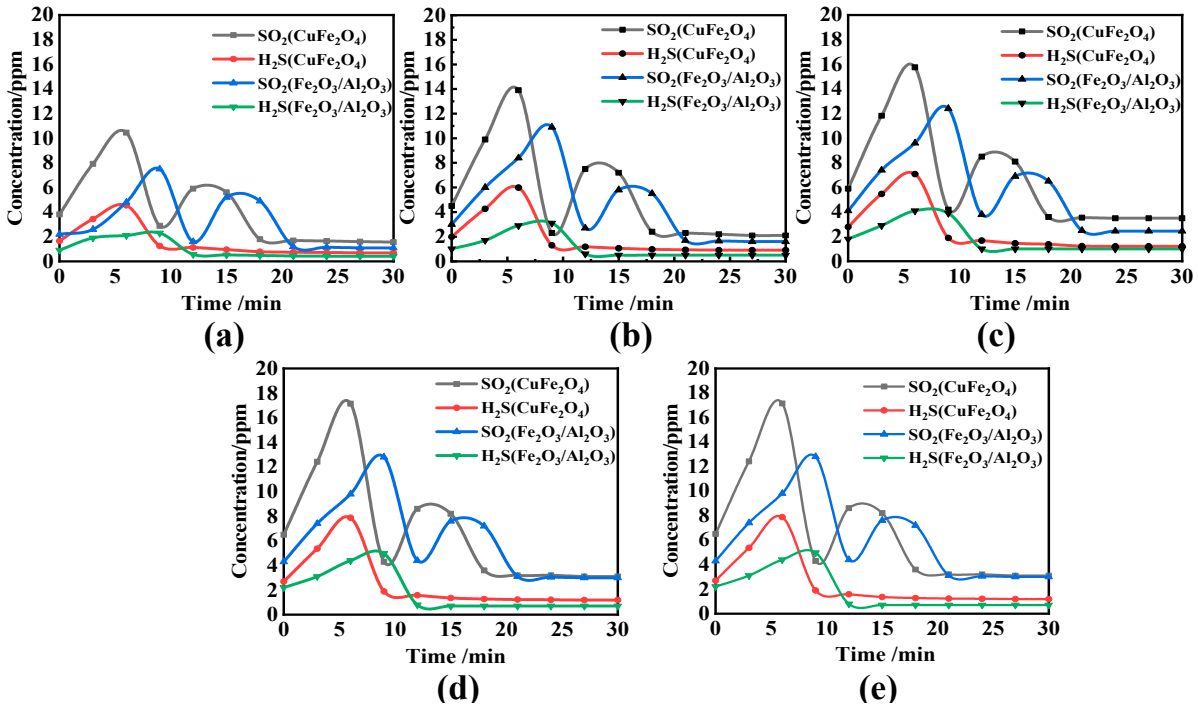

Figure 6. The variation trend of SO_2 and H_2S with time in the process of CLC at (**a**) 650 °C, (**b**) 700 °C, (**c**) 750 °C, (**d**) 800 °C and (**e**) 850 °C.

The NOx precursors HCN and NH_3 were not detected in the reaction process. Because OC particles had a strong oxidation effect, the nitrogen-containing precursor could be oxidized to N_2 and NOx [15,16,26,27]. Therefore, the trend of HCN and NH_3 could be speculated by the trend of NOx. NO showed a basic trend of bimodal release during the reaction, and its release amount increased with the increase in the reaction temperature, as shown in Figure 7. The reason for this phenomenon is similar to the formation mechanism of SO_2. It is worth noting that $CuFe_2O_4$ can release both molecular oxygen and lattice oxygen. Therefore, compared with iron-based, OC $CuFe_2O_4$ has stronger oxidation effects on HCN and NH_3, which can be converted into higher-valence NO and NO_2 rather than released in the form of N_2. With the increase in reaction temperature, the content of NO_2 basically stayed the same, which may be due to the thermodynamic limitation of the conversion process of HCN and NH_3 to NO_2, resulting in no obvious change in NO_2 with temperature. According to the thermodynamic simulation results, similar phenomena were

also found and the change trend of NO with temperature was more obvious than that of NO_2.

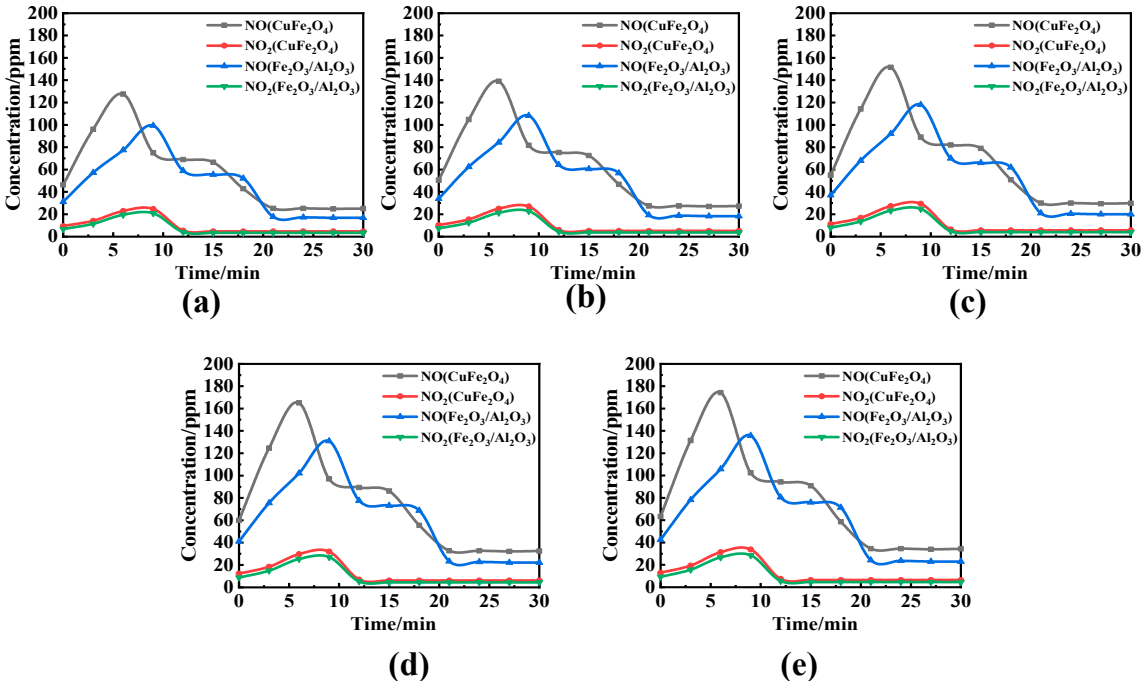

Figure 7. The variation trend of NO and NO_2 with time in the process of CLC at (**a**) 650 °C, (**b**) 700 °C, (**c**) 750 °C, (**d**) 800 °C and (**e**) 850 °C.

When the temperature was set to 850 °C, as shown in Figure 8, with the increase in O/C, the content of SO_2 and H_2S increased. An increase in O/C can promote the CLC reaction, which made the contact between OC particles and coal particles more intense, and helped to release gaseous sulfur. A high O/C also means that OC can release more O_2/lattice oxygen [21,28], which can effectively promote the gasification reaction of coal char and promote the decomposition of coal char particles to release H_2S and generate SO_2. However, with the increase in O/C, the content of NO and NO_2 has no obvious change, and OC particles have little effect on the migration and transformation characteristics of fuel nitrogen, which was mainly caused that solid–solid reaction was difficult to carry on between coal and oxygen carrier particles [11,19,27]. It can be seen in Figure 9 that NO and NO_2 released a lot in the pyrolysis stage of coal. Although NO and NO_2 are also produced in the gasification stage, their contents were relatively small. Most aromatic nitrogen-containing compounds in coal were released in large quantities in the pyrolysis stage due to their thermodynamic instability, resulting in insufficient contact between OC particles and nitrogen-containing products being taken out of the reactor [11,17]. Therefore, NO and NO_2 cannot change significantly with the increase in O/C.

First of all, the increase in the reaction temperature can promote the release of sulfur and nitrogen pollutants in coal by promoting the decomposition of coal particles. Secondly, different oxygen release modes of OC particles have different effects on the migration and transformation behavior of sulfur and nitrogen in coal. The release of molecular oxygen from $CuFe_2O_4$ can promote the conversion of fuel nitrogen to higher-valence NOx. At the same time, due to the presence of the copper phase in OC, it can easily interact with H_2S, and the formation of Cu_2S leads to sulfur poisoning, as shown in Figure 10b. However, with the increase in O/C and temperature, the sulfur poisoning phenomenon of $CuFe_2O_4$ is gradually weakened, and the contents of SO_2 and H_2S in flue gas are significantly increased.

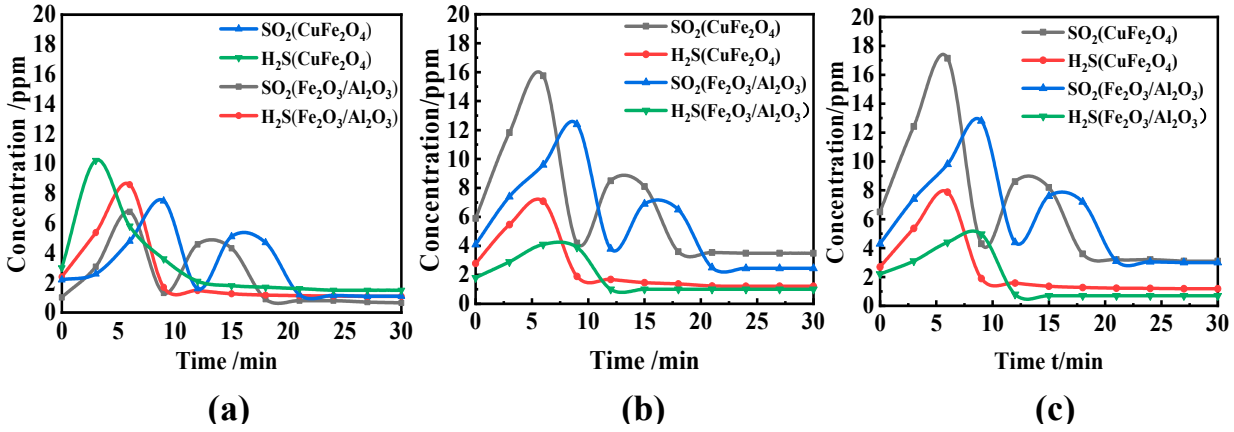

Figure 8. The variation trend of H_2S and SO_2 with time in the process of CLC at (**a**) O/C = 1, (**b**) O/C = 3 and (**c**) O/C = 5 in 850 °C.

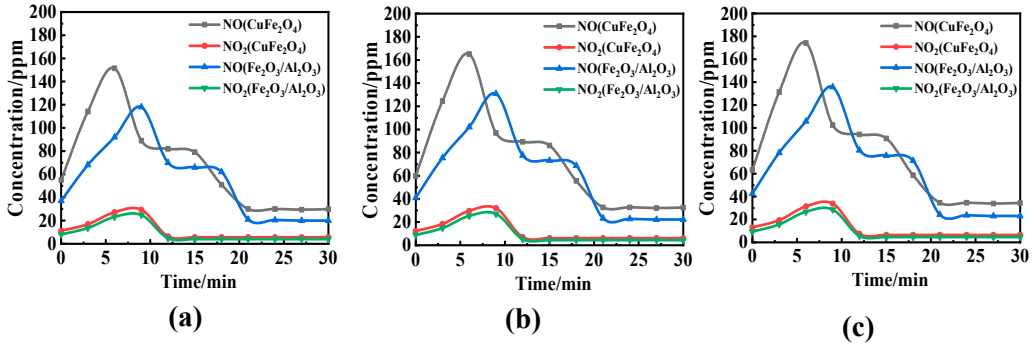

Figure 9. The variation trend of NO and NO_2 with time in the process of CLC at (**a**) O/C = 1, (**b**) O/C = 3 and (**c**) O/C = 5 in 850 °C.

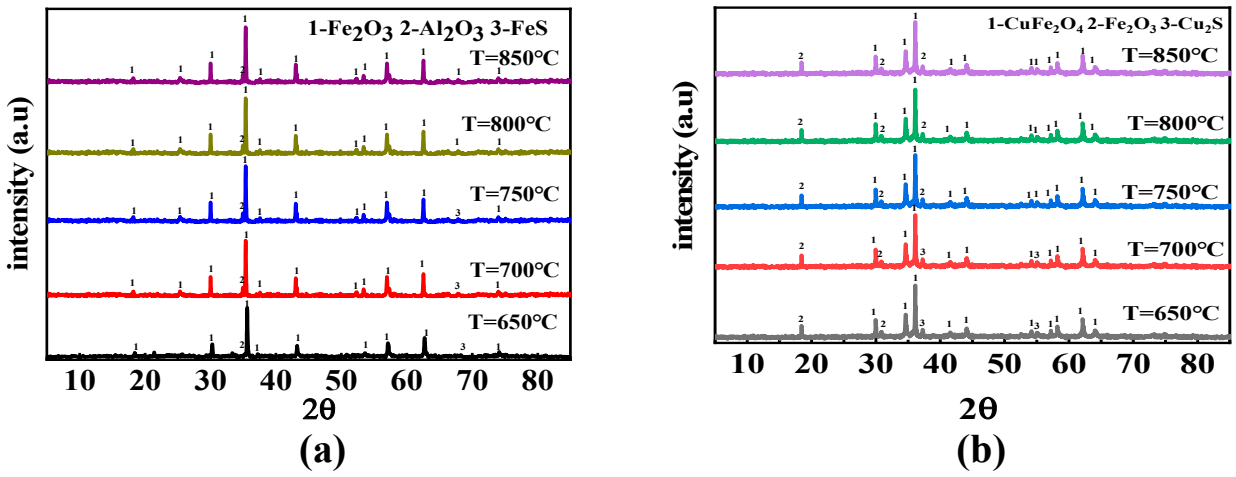

Figure 10. XRD patterns of (**a**) Fe_2O_3/Al_2O_3 and (**b**) $CuFe_2O_4$ at different reaction temperatures.

3.3. Transformation and Migrant Behavior of Sulfur and Nitrogen in Cyclic Experiment

In this section, the effects of O/C and reaction temperature on the migration and transformation mechanism of sulfur and nitrogen were discussed during CLC. When the reaction temperature was 850 °C and O/C = 5, the promotion effect of iron-based OC and $CuFe_2O_4$ on sulfur and nitrogen was obvious. On this basis, 10 cycles were carried out. With the increase in cycles, the contents of H_2S, SO_2 and NOx in flue gas gradually increased, as shown in Figures 11 and 12. According to Table 2, it can be found that the

BET specific surface area of the two types of OC increased gradually with the increase in the number of cycles. The increase in the specific surface area of the OC can promote the transformation of oxygen between the fuel and the OC, resulting in the increase in the concentration of the product layer on the surface of the OC, and the reaction on the surface of the OC was intensified. To a certain extent, it promoted the decomposition of coal particles and the release of sulfur and nitrogen pollutants in the fuel. On the other hand, as the number of cycles increases, the OC particles may be inactivated, resulting in a decrease in the fixation of sulfur and nitrogen pollutants in flue gas by OC. The XRD patterns of iron-based OC and $CuFe_2O_4$ after 10 cycles are shown in Figure 13 [26]. With the increase in cycles, the OC particles does not show the phase separation phenomenon and can still maintain a relatively complete crystal phase. However, the increase in cycle times leads to a decrease in the peak intensity of the XRD pattern of $CuFe_2O_4$ [13], which means that the content of effective components in OC decreases. Therefore, the interaction between $CuFe_2O_4$ and sulfur gradually decreases with the increase in cycle number, and the content of SO_2 and H_2S in flue gas is significantly higher than that of iron-based OC.

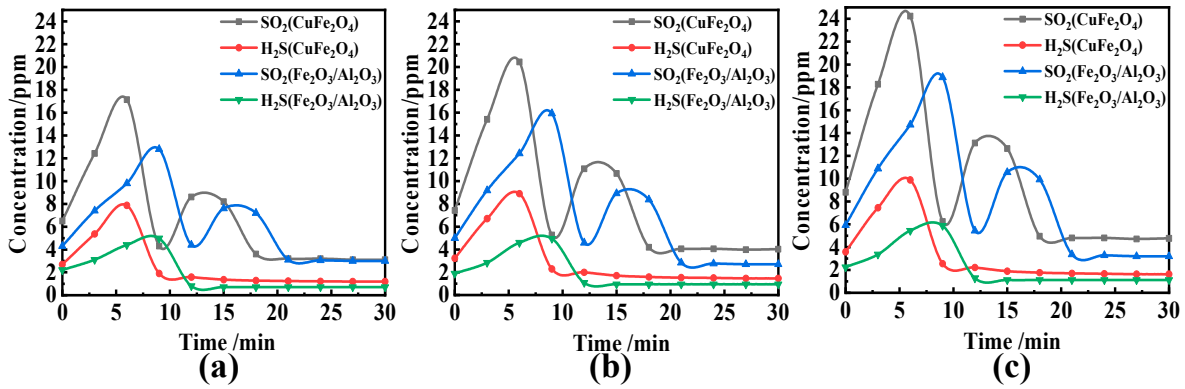

Figure 11. Trends of SO_2 and H_2S over time during reduction using iron-based OC and $CuFe_2O_4$ as OC in (**a**) 1st, (**b**) 5th and (**c**) 10th cyclic experiments.

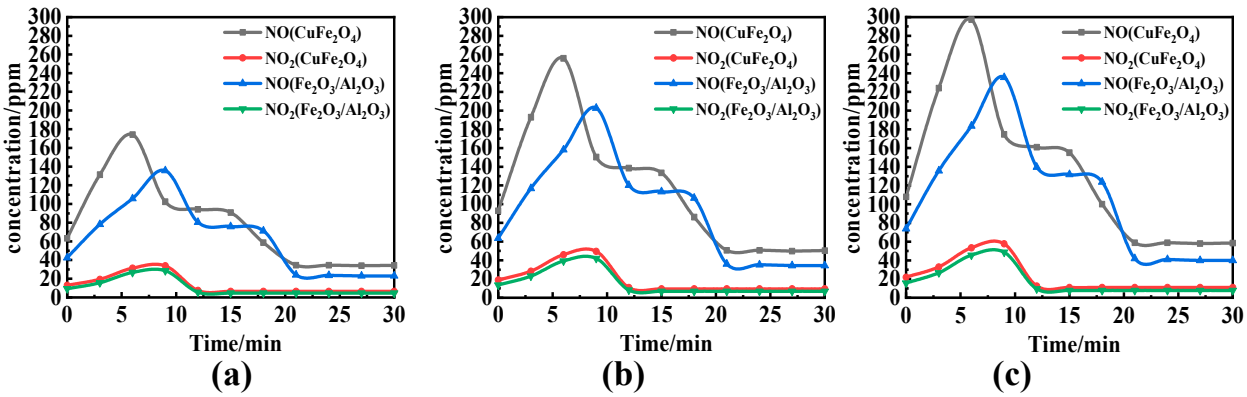

Figure 12. Trends of NO and NO_2 over time during reduction using iron-based oxygen carriers and $CuFe_2O_4$ as OC in (**a**) 1st, (**b**) 5th and (**c**) 10th cyclic experiments.

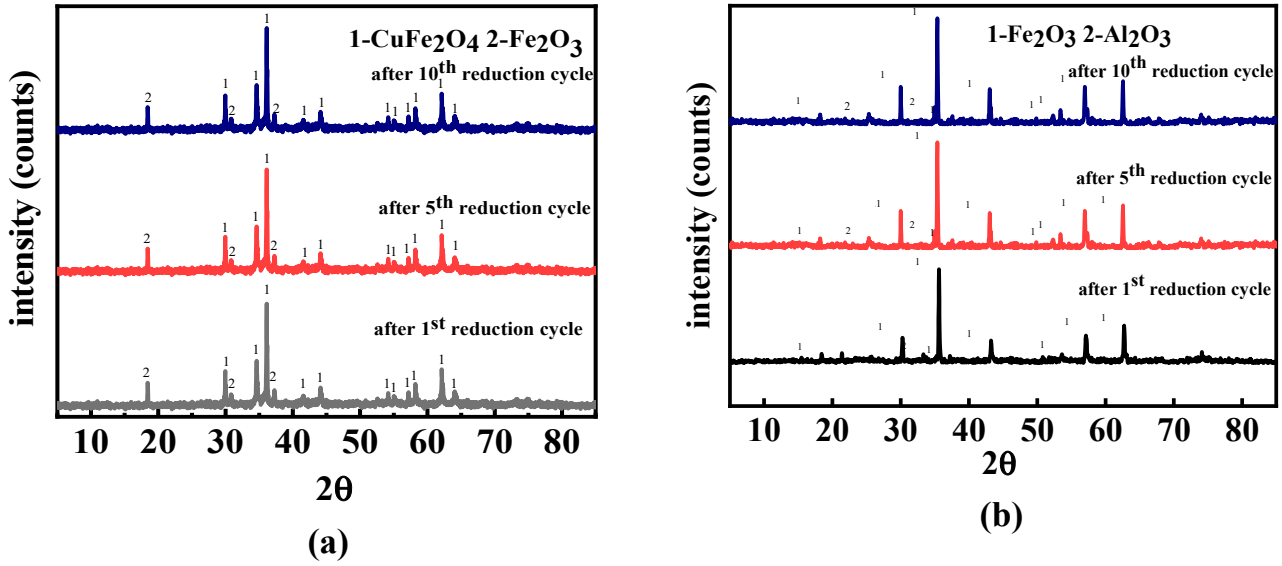

Figure 13. XRD patterns of (**a**) Fe_2O_3/Al_2O_3 and (**b**) $CuFe_2O_4$ in different cyclic experiments.

Table 2. BET (Brunauer, Emmett, and Teller) specific surface area of $CuFe_2O_4$ and iron-based OC after cyclic experiment.

Sample	$S_{BET}/(m^2/g)$ of $CuFe_2O_4$	$S_{BET}/(m^2/g)$ of Fe_2O_3/Al_2O_3
Fresh	2.339	1.872
After 1st	5.101	4.446
After 5th	5.576	4.782
After 10th	6.475	5.020

3.4. Reaction Characteristics of CLC

A higher reaction temperature and higher O/C can promote the release of sulfur and nitrogen pollutants during CLC [18,27,28]. The reaction characteristics of NX coal during CLC were investigated in a fluidized bed reactor at 850 °C and O/C = 5, and the results are shown in Figure 14. During the reaction, the outlet concentrations of CH_4, CO and CO_2 gradually increased with the increase in reaction time, and the outlet concentrations of CO_2 were 90.55% and 98.75% when iron-based OC and $CuFe_2O_4$ were used. Therefore, because of its good oxygen release ability and good reactivity, $CuFe_2O_4$ can obtain a higher concentration of CO_2 in the same reaction time compared with iron-based OC, which was more suitable for CO_2 capture during CLC. $CuFe_2O_4$ still showed excellent reaction characteristics in the same reaction time, the conversion ability of carbon-based material was stronger, and the yield of per unit time of CO_2 ($dxCO_2$) was higher, as shown in Figure 14d.

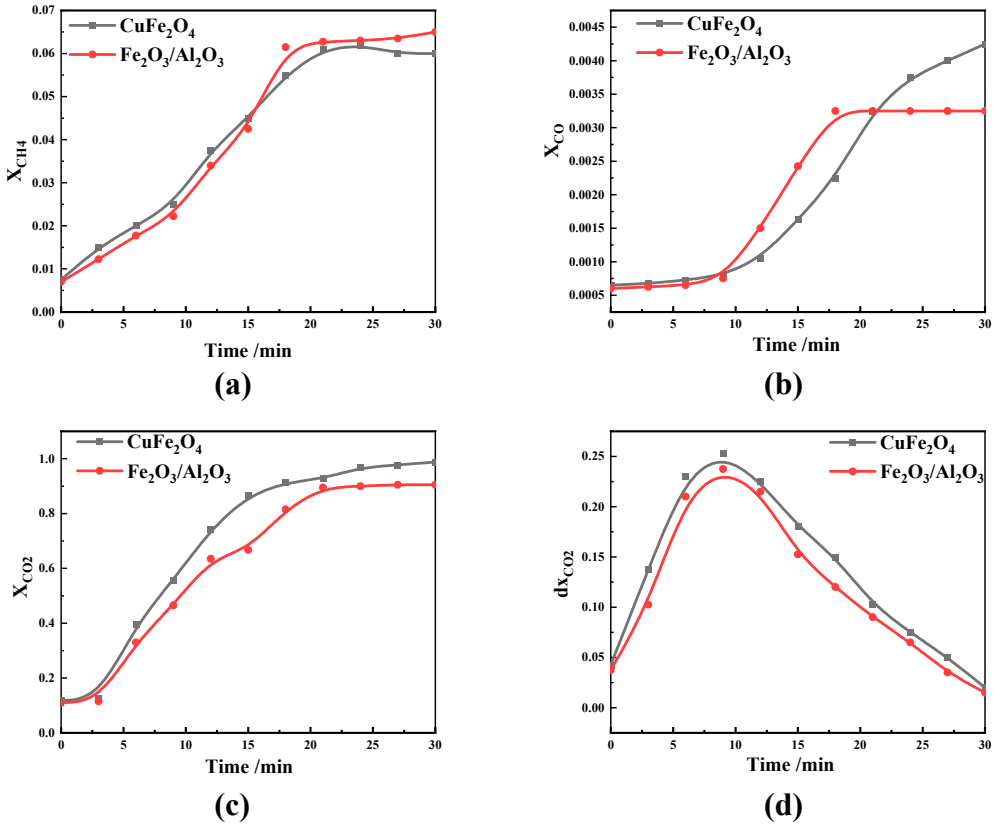

Figure 14. Trend of (**a**) CH_4, (**b**) CO, (**c**) CO_2 and (**d**) dx_{CO2} over time of iron-based OC and $CuFe_2O_4$ during CLC.

4. Conclusions

In the process of CLC, the migration and transformation mechanism of sulfur and nitrogen elements with NX coal and two kinds of OC were systematically explored in fluidized bed reactor, and the mechanism of different OC on sulfur and nitrogen was simulated by thermodynamic simulation software, HSC Chemistry 6.0. On this basis, the effects of O/C, reaction temperature and cycle number on the migration and transformation behaviors of sulfur and nitrogen were expounded.

1. Different OC have different effects on CO, CH_4 and CO_2 at the same O/C and reaction temperature. $CuFe_2O_4$ contains both iron and copper phases, and so has the dual advantages of Fe_2O_3 and CuO. It can simultaneously release molecular oxygen and lattice oxygen, and has good oxygen release characteristics and reaction characteristics. Compared with iron-based OC, it is easier to obtain a high concentration of CO, which is more suitable for CLC.
2. H_2S increased first and then decreased in the reaction process, and a lot was released in the coal pyrolysis stage, while SO_2 showed a bimodal release trend. Compared with solid–solid reactions, $CuFe_2O_4$ can release molecular oxygen. A gas–solid reaction is more likely to occur. Therefore, $CuFe_2O_4$ can promote the release of H_2S and SO_2, and its promotion effect on H_2S and SO_2 is still obvious with the increase in O/C and reaction temperature. Based on the thermodynamic simulation and experimental results, when the reaction temperature is higher than 800 °C, $CuFe_2O_4$ can resist sulfur poisoning. Therefore, an appropriate reaction temperature can not only inhibit OC particles sulfur poisoning, but also promote combustion characteristics.
3. Considering nitrogen in coal, the content of NOx in flue gas increased significantly when OC released molecular oxygen, and the content of NO and NO_2 increased with the increase in reaction temperature. The effect of O/C on NOx in flue gas was not obvious, and with the increase in O/C the content of NOx did not change

obviously. Therefore, the oxygen release mode of OC only affects the conversion of the fuel nitrogen valence state. The oxygen decoupling oxygen carrier can convert fuel nitrogen into NO and NO_2, so that CLC is similar to the traditional combustion process. Iron-based OC can convert fuel nitrogen into N_2 instead of releasing fuel nitrogen in the form of NOx. Therefore, Fe_2O_3/Al_2O_3 can release lattice oxygen and is more suitable for CLC with a high content nitrogen of coal, which can convert fuel nitrogen into N_2 release and reduce NOx release.

Supplementary Materials: The following supporting information can be downloaded at: https://www.mdpi.com/article/10.3390/atmos13050786/s1, **Figure S1**: The fluidized bed reactor used in experiment; **Figure S2**: (a) Gasmet gas analyzer (b) VARIO Plus MRU gas analyzer.

Author Contributions: Conceptualization, J.M. and Q.G.; data curation, J.M., H.L. and Q.G.; investigation, C.H. and Z.H.; methodology, C.H. and Z.H.; resources, H.L.; writing—original draft, J.M. and H.L.; writing—review and editing, H.L. All authors have read and agreed to the published version of the manuscript.

Funding: The authors are grateful for the financial support for the following projects: the Key Research and Development Program Project of Ningxia (2018BEE03009) and the National First-rate Discipline Construction Project of Ningxia (NXYLXK2017A04).

Institutional Review Board Statement: Not applicable.

Informed Consent Statement: Not applicable.

Data Availability Statement: Not applicable.

Conflicts of Interest: The authors declare no competing financial interest.

References

1. Saqline, S.; Chua, Z.Y.; Liu, W. Coupling chemical looping combustion of solid fuels with advanced steam cycles for CO_2 capture: A process modelling study. *Energy Convers. Manag.* **2021**, *244*, 114455. [CrossRef]
2. Abuelgasim, S.; Wang, W.; Abdalazeez, A. A brief review for chemical looping combustion as a promising CO_2 capture technology: Fundamentals and progress. *Sci. Total Environ.* **2021**, *764*, 142892. [CrossRef] [PubMed]
3. Zhao, H.; Tian, X.; Ma, J.; Chen, X.; Su, M.; Zheng, C.; Wang, Y. Chemical looping combustion of coal in China: Comprehensive progress, Remaining Challenges, and Potential Opportunities. *Energy Fuels* **2020**, *34*, 6696–6734. [CrossRef]
4. Adánez-Rubio, I.; Abad, A.; Gayán, P.; García-Labiano, F.; Luis, F.; Adánez, J. The fate of sulphur in the Cu-based Chemical Looping with Oxygen Uncoupling (CLOU) Process. *Appl. Energy* **2014**, *113*, 1855–1862. [CrossRef]
5. Linderholm, C.; Schmitz, M. Chemical-looping combustion of solid fuels in a 100 kW dual circulating fluidized bed system using iron ore as oxygen carrier. *J. Environ. Chem. Eng.* **2016**, *4*, 1029–1039. [CrossRef]
6. Adánez, J.; Abad, A.; Mendiara, T.; Gayán, P.; De Diego, L.F.; García-Labiano, F. Chemical looping combustion of solid fuels. *Prog. Energy Combust. Sci.* **2018**, *65*, 6–66. [CrossRef]
7. Zhao, H.; Tian, X.; Ma, J.; Su, M.; Wang, B.; Mei, D. Development of tailor-made oxygen carriers and reactors for chemical looping processes at Huazhong University of Science & Technology. *Int. J. Greenh. Gas Control* **2020**, *93*, 102898.
8. Wang, P.; Howard, B.; Means, N. Investigation of reactivities of bimetallic Cu-Fe oxygen carriers with coal in high temperature in-situ gasification chemical-looping combustion (iG-CLC) and chemical-looping with oxygen uncoupling (CLOU) using a fixed bed reactor. *Fuel* **2021**, *285*, 119012. [CrossRef]
9. Zhu, X.; Shen, T.; Bollas, G.; Shen, L. Design and operation of a multi-stage reactor system for chemical looping combustion process. *Fuel Process. Technol.* **2021**, *215*, 106748. [CrossRef]
10. Wen, C.; Yu, D.; Wang, J.; Wu, J.; Yao, H.; Xu, M. Effect of the devolatilization process on PM10 Formation during oxy-fuel combustion of a typical bituminous coal. *Energy Fuels* **2014**, *28*, 5682–5689. [CrossRef]
11. Song, T.; Shen, L.; Xiao, J.; Chen, D.; Gu, H.; Zhang, S. Nitrogen transfer of fuel-N in chemical looping combustion. *Combust. Flame* **2012**, *159*, 1286–1295. [CrossRef]
12. Izquierdo, M.T.; García-Labiano, F.; Abad, A.; Cabello, A.; Gayán, P.; de Diego, L.F.; Adánez, J. On the optimization of physical and chemical stability of a Cu/Al_2O_3 impregnated oxygen carrier for chemical looping combustion. *Fuel Process. Technol.* **2021**, *215*, 106740. [CrossRef]
13. Pachler, R.F.; Mayer, K.; Penthor, S.; Kollerits, M.; Hofbauer, H. Fate of sulfur in chemical looping combustion of gaseous fuels using a copper-based oxygen carrier. *Int. J. Greenh. Gas Control* **2018**, *71*, 86–94. [CrossRef]
14. Wang, B.; Yan, R.; Zhao, H.; Zheng, Y.; Liu, Z.; Zheng, C. Investigation of chemical looping combustion of coal with $CuFe_2O_4$ oxygen carrier. *Energy Fuels* **2011**, *25*, 3344–3354. [CrossRef]

15. Fan, B.; Wen, C.; Zeng, X.; Wu, J.; Yu, X. Emission Behaviors of Inorganic Ultrafine Particles during Zhundong Coal Oxy-Fuel Combustion with Characterized Oxygen Input Fractions Comparable to Air Combustion. *Appl. Sci.* **2018**, *8*, 1486. [CrossRef]
16. Luo, M.; Zhou, L.; Cai, J.; Zhang, H.; Wang, C. Migration of sulfur in in-situ gasification chemical looping combustion of Beisu coal with iron-and copper-based oxygen carriers. *Chin. J. Chem. Eng.* **2021**, *35*, 247–255.
17. Mendiara, T.; Izquierdo, M.T.; Abad, A.; De Diego, L.F.; García-Labiano, F.; Gayán, P.; Adánez, J. Release of pollutant components in CLC of lignite. *Int. J. Greenh. Gas Control* **2014**, *22*, 15–24. [CrossRef]
18. Ma, J.; Mei, D.; Wang, C.; Tian, X.; Liu, Z.; Zhao, H. Sulfur fate during in-situ gasification chemical looping combustion (iG-CLC) of coal. *Chem. Eng. J.* **2021**, *406*, 126773. [CrossRef]
19. Song, T.; Shen, T.; Shen, L.; Xiao, J.; Gu, H.; Zhang, S. Evaluation of hematite oxygen carrier in chemical-looping combustion of coal. *Fuel* **2013**, *104*, 244–252. [CrossRef]
20. Pérez-Vega, R.; Adánez-Rubio, I.; Gayán, P.; Izquierdo, M.T.; Abad, A.; García-Labiano, F.; Luis, F.; Adánez, J. Sulphur, nitrogen and mercury emissions from coal combustion with CO_2 capture in chemical looping with oxygen uncoupling (CLOU). *Int. J. Greenh. Gas Control* **2016**, *46*, 28–38. [CrossRef]
21. Ishida, M.; Jin, H. A novel chemical-looping combustor without NOx formation. *Ind. Eng. Chem. Res.* **1996**, *35*, 2469–2472. [CrossRef]
22. An, M.; Ma, J.; Guo, Q. Transformation and migration of mercury during chemical-looping gasification of coal. *Ind. Eng. Chem. Res.* **2019**, *58*, 20481–20490. [CrossRef]
23. Adánez-Rubio, I.; Gayán, P.; García-Labiano, F.; Luis, F.; Adánez, J.; Abad, A. Development of CuO-based oxygen-carrier materials suitable for Chemical-Looping with Oxygen Uncoupling (CLOU) process. *Energy Procedia* **2011**, *4*, 417–424. [CrossRef]
24. Wang, C.; Luo, M.; Zhou, L.; Zhang, H. Sulfur Transformation Behavior of Inorganic Sulfur-Containing Compounds in Chemical Looping Combustion. *Energy Fuels* **2020**, *34*, 3969–3975. [CrossRef]
25. Ma, J.; Tian, X.; Wang, C.; Zhao, H.; Liu, Z.; Zheng, C. Fate of fuel-nitrogen during in situ gasification chemical looping combustion of coal. *Fuel Process. Technol.* **2021**, *215*, 106710. [CrossRef]
26. Chung, C.; Pottimurthy, Y.; Xu, M.; Hsieh, T.; Xu, D.; Zhang, Y.; Chen, Y.; He, P.; Pickarts, M.; Fan, L.; et al. Fate of sulfur in coal-direct chemical looping systems. *Appl. Energy* **2017**, *208*, 678–690. [CrossRef]
27. Gu, H.; Shen, L.; Zhong, Z.; Niu, X.; Ge, H.; Zhou, Y.; Xiao, S.; Jiang, S. NO release during chemical looping combustion with iron ore as an oxygen carrier. *Chem. Eng. J.* **2015**, *264*, 211–220. [CrossRef]
28. Chen, P.; Gu, M.; Chen, G.; Huang, X.; Lin, Y. The effect of metal calcium on nitrogen migration and transformation during coal pyrolysis: Mass spectrometry experiments and quantum chemical calculations. *Fuel* **2020**, *264*, 116814. [CrossRef]